GEOPHYSICAL RESEARCH LETTERS, VOL. 28, NO. 11, PAGES 2169-2172, JUNE 1, 2001

Solar Cycle Variations in the Electron Heat Flux: Ulysses Observations

Earl E. Scime, and J. E. Littleton
West Virginia University, Morgantown, West Virginia

S. Peter Gary and Ruth Skoug
Los Alamos National Laboratory, Los Alamos, New Mexico

Naiguo Lin
University of Minnesota, Minneapolis, Minnesota

Abstract. Solar wind observations by the Ulysses spacecraft now include nearly ten years of continuous ion and electron measurements. In this study, we report detailed measurements of the electron heat flux in the solar wind. In particular, we examine the heat flux measurements for long-term correlations with wave activity and solar wind speed. We find that the average heat flux, when scaled by $R^{2.9}$ to account for variations due to distance from the Sun, is constant and independent of heliographic latitude or solar cycle. We find that during both solar maximum and solar minimum, there is no significant correlation between the magnitude of the electron heat flux and the solar wind speed. Comparison of the electron heat flux data with wave activity indicates that the whistler heat flux instability does not play an important role in limiting the solar wind heat flux.

1. Introduction

As part of a long-term investigation of the role played by electron heat conduction in the expansion of the solar wind, nearly ten years of data from the Ulysses spacecraft are examined for correlations between electron heat flux, solar wind speed, heliographic latitude, and wave activity. Discussion of the scientific questions raised by the magnitude of the electron heat flux in the solar wind can be found in *Scime et al.* [1994b] and *Scudder and Olbert* [1979a, b].

The Ulysses mission was specifically designed to examine the detailed properties of the solar wind from a circumpolar orbit. The ten-year span of the Ulysses mission now includes an in-ecliptic phase from 1 to 5 AU during solar minimum, a complete polar orbit during solar minimum, and the incoming portion of a polar orbit during solar maximum. Previous studies of electron heat flux measurements obtained by Ulysses have shown that in the ecliptic, the magnitude of the electron heat flux obeys a $R^{-2.9}$ scaling (where R is the heliocentric distance of the spacecraft) [*Scime et al.*, 1994b]. The $R^{-2.9}$ scaling of the electron heat flux from 1 to 5 AU observed by Ulysses is consistent with Helios measurements from within 1 AU [*Pilipp et al.*, 1987]. In the absence of any regulatory mechanism and without an ambient magnetic field, the magnitude of the electron heat flux should fall of as R^{-2} [*Scime et al.*, 1994b]. This calculation assumes a negligible effect of the interplanetary potential on the magnitude of the electron heat flux [*Scudder and Olbert*, 1979a, b]. When the effects of the spiral magnetic field are included, the radial scaling of the electron heat flux magnitude becomes even shallower than R^{-2} [*Scime et al.*, 1994b]. Thus, the in-ecliptic measurements suggest the action of some mechanism that actively dissipates or regulates the electron heat flux as the solar wind expands.

Because the radial scaling of the electron heat flux is consistent with the predicted radial scaling of an electron heat flux threshold instability ($q_e \sim R^{-3.0}$) [*Gary et al.*, 1994; *Scime et al.* 1994b], there have been a number of studies that have examined the correlation between electron heat flux magnitude and wave activity in the solar wind [*Lin et al.*, 1998, *Newbury and Gary*, 2001]. A recent computational model that uses experimental data for constraints at 1 AU and includes the possibility of an electron heat flux dissipation mechanism also yields a radial scaling for the electron heat flux consistent with the observations [*Sittler and Guhathakurta*, 1999]. However, apart from intervals near shocks and strong stream interfaces [*Lin et al.*, 1998], there have been no clear indications of a correlation between electron heat flux magnitude and wave activity [*Newbury and Gary*, 2001].

A key feature of models that rely on the action of the interplanetary potential to reduce the electron heat flux is the relationship between the solar wind speed and the magnitude of the electron heat flux [*Hollweg* 1974; *Scudder and Olbert*, 1979a, b]. Some of the models predict that the wind speed and electron heat flux should be locally anti-correlated [*Scudder and Olbert*, 1979a, b], while others suggest that the presence of a suprathermal tail in the electron distribution provides sufficient energy to drive high solar wind speeds (> 600 km/s) [*Maksimovic et al.*, 1997; *Meyer-Vernet*, 1999]. Given the dramatic change in solar wind speed from low latitude to high latitude during solar minimum (400 km/s to 800 km/s) [*McComas et al.*, 2001a], these models predict a quantifiable change in the magnitude of the electron heat flux should be observed as the Ulysses spacecraft moves from the low-speed into the high-speed solar wind. However, data from the polar orbit during solar minimum indicated no correlation between the electron heat flux and heliographic latitude [*Scime et al.*, 1999].

In this paper, we report our analysis of nearly ten years of electron heat flux measurements from the Ulysses spacecraft. In the following sections the instruments used are described and the results of our analysis are presented and discussed.

Paper number 2001GL012925
0094-8276/01/2001GL012925$05.00

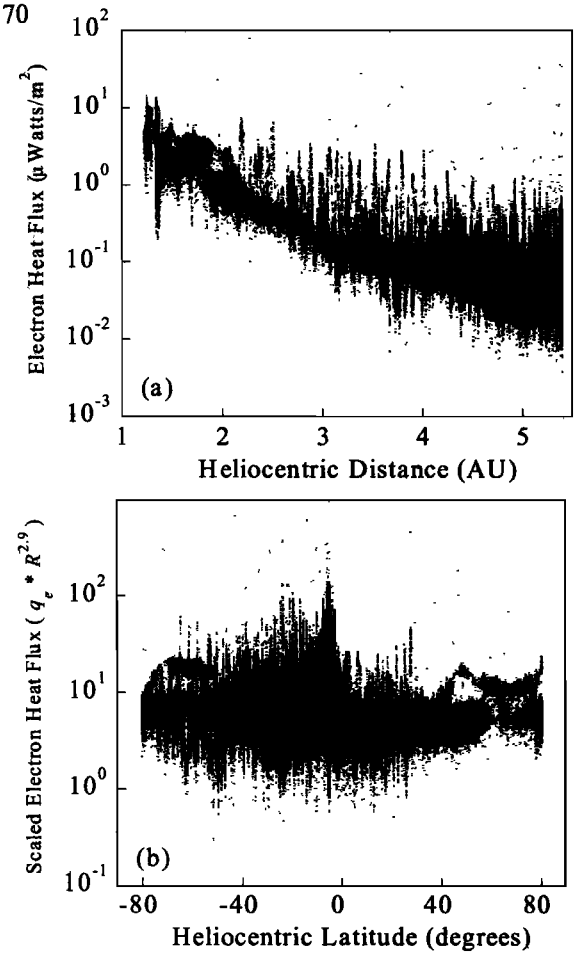

Figure 1. (a) Electron heat flux versus heliocentric distance for all ten years of the Ulysses mission. (b) Electron heat flux scaled by $R^{2.9}$ versus heliographic latitude.

2. Instruments

During the in-ecliptic phase of the Ulysses mission, three-dimensional measurements of the solar wind electron distributions were obtained with the Solar Wind Observations Over the Poles of the Sun (SWOOPS) electron instrument [*Bame et al.*, 1992]. One out of every three spectra returned is fully three-dimensional in velocity space. We have used three-dimensional phase space densities exclusively in this study and have corrected the data for spacecraft charging effects [*Scime et al.*, 1994a] and a high latitude light leak [*Scime et al.*, 1999]. In addition, electron data for which the calculated electron density differs significantly from the ion instrument density measurements have been excluded. Numerical integrations of the electron distributions in the rest frame of the distribution are used to calculate the electron heat flux.

$$q_e = \int \frac{m}{2} \mathbf{U} U^2 f_e d^3 v \qquad (1)$$

where $\mathbf{U} = \mathbf{v} - \langle \mathbf{v} \rangle$, and $\langle \mathbf{v} \rangle$ is the average electron velocity. In the ecliptic, the field aligned halo electrons are responsible for the majority of the electron heat flux [*Scime et al.*, 1994b]. The proton speeds used in this study were obtained with the SWOOPS ion instrument [*Bame et al.*, 1992]. The waveform analyzer (WFA) wave data used in this study was obtained with the Unified RAdio and Plasma (URAP) wave instrument [*Stone et al.*, 1992]. The WFA provides spectral analysis of electric and magnetic signals in a frequency range between 0.22 and 448 Hz.

3. Correlations with Distance, Latitude, Solar Cycle, and Wave Activity

Ten years of electron heat flux magnitude measurements are shown as a function of heliographic distance in Figure 1a. The large variations in electron heat flux magnitude occur at shocks and high-to-low solar wind speed interfaces. A power law fit to the entire data set yields a radial scaling for the electron heat flux of $q_e = 7.4\, R^{-2.9}$ μWatts/m^2. Both the magnitude and exponent of the fit are nearly identical with the in-ecliptic results [*Scime et al.*, 1994b]. The same data scaled by $R^{2.9}$ is plotted versus heliographic latitude in Figure 1b. A linear fit to the scaled data versus latitude yields an almost perfectly flat line. Thus, there is no significant variation of the electron heat flux with latitude that cannot be attributed to the radial variation observed in the ecliptic during solar minimum.

In Figure 2, the electron heat flux versus latitude is shown separately for solar minimum (Figure 2a) and solar maximum (Figure 2b). For the purposes of this study, solar minimum includes the years 1991 through 1997 while solar maximum includes the years 1998 through 2001. The end of 1997 was chosen to correspond to the beginning of Ulysses' second solar polar orbit. A striking difference in the two data sets is the variations in electron heat flux at high latitude during solar maximum. The high latitude solar wind speed is also markedly different during these two phases of the solar cycle. Instead of increasing from roughly 400 km/s to 900 km/s as Ulysses traveled from low latitude to high latitude, the average solar wind speed during this solar maximum polar transit has remained nearly constant at 400 km/s [*McComas et*

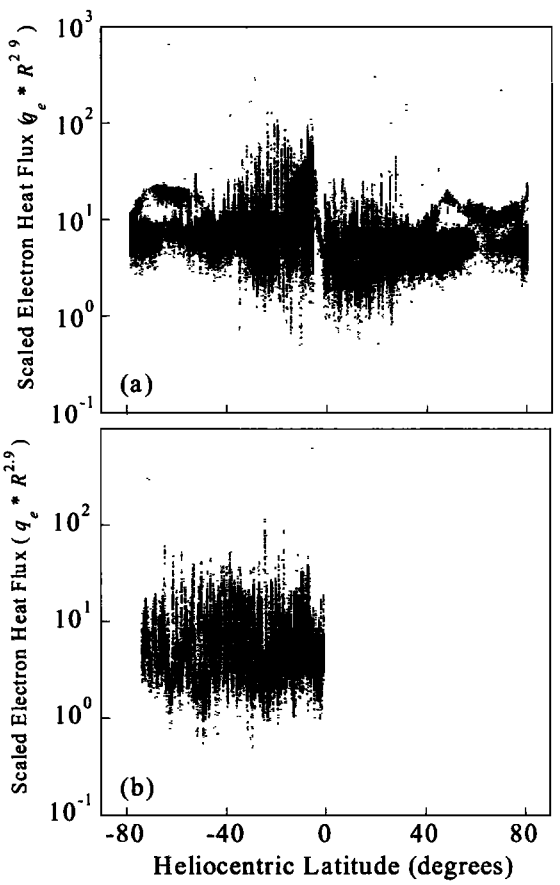

Figure 2. (a) Electron heat flux scaled by $R^{2.9}$ versus heliographic latitude during (a) solar minimum (1990 – 1997) and (b) solar maximum (1998 – 2001).

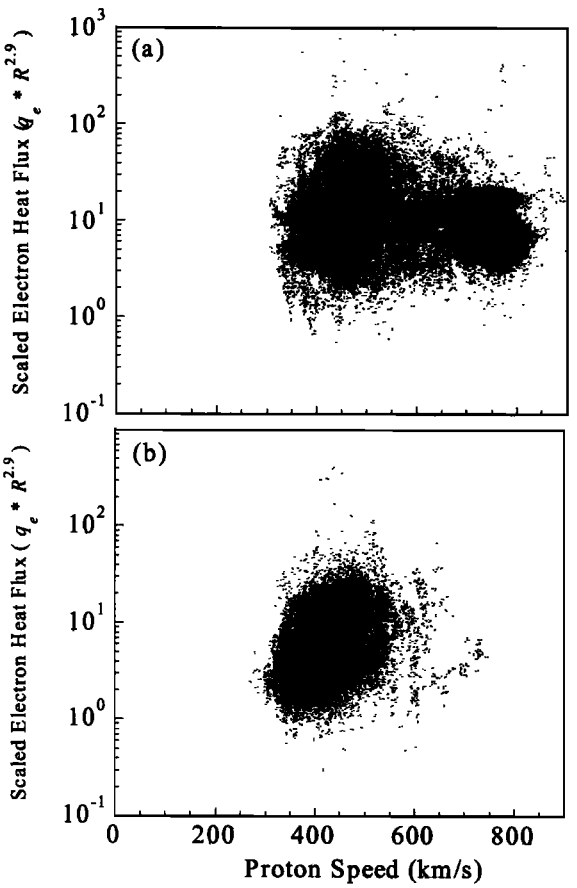

Figure 3. Electron heat flux scaled by $R^{2.9}$ versus proton speed for the latitude range 0° to –75° during (a) solar minimum and (b) solar maximum.

al., 2001b]. Variations in the solar wind speed, on the order of + 200 km/s, continue to occur and are strongly correlated with the variations in electron heat flux that are apparent in Figure 2b. An unexplained feature in the solar minimum data is the bi-modal nature of the electron heat flux at high latitude. This appears as a pair of "peaked" lines above the baseline electron heat flux data at high latitude in Figure 2a. Careful examination of the raw data and the absence of this feature during solar maximum (Figure 2b) suggest that this feature is not an instrumental artifact. However, we continue to examine the solar minimum data for possible evidence that the bi-modal feature is artificially generated during the analysis process. Other electron parameters, such as the electron temperature, also vary over a wider range in the low speed, high latitude, solar wind characteristic of solar maximum than in the high speed, high latitude, solar wind observed during solar minimum.

The scaled electron heat flux versus proton speed is shown in Figure 3a for latitudes of 0° to –75° during solar minimum. The data is clearly divided into two different solar wind states, the low latitude solar wind ($V \sim 400$ km/s) and the high latitude solar wind ($V \sim 800$ km/s) emanating from the coronal hole. At the higher solar wind speeds, the bi-modal feature in the electron heat flux mentioned previously is apparent. Although there is less variability in the electron heat flux in the high-speed wind, there does not appear to be any significant correlation between solar wind speed and electron heat flux. This result does not contradict the observation of a correlation between solar wind speed and the ratio of halo to core kinetic pressures as reported in *Maksimovic et al.* [2001]. The ratio of kinetic pressures does not depend on the relative velocity of the core and halo components and therefore is not representative of the electron heat flux. Data for the same latitude range is shown in Figure 3b for solar maximum. The log-linear nature of Figure 3b overemphasizes a very weak correlation between solar wind speed and electron heat flux, i.e., larger values of electron heat flux are observed at higher solar wind speeds. Clear decreases in electron heat flux magnitude during periods of decreasing solar wind speed were observed during short time scale, rapid decreases in solar wind speed during solar minimum [*Lin et al.*, 1998]. Because the electron heat flux does not increase as the average wind speed doubles during solar minimum (Figure 3a), the very weak correlation between solar wind speed and electron heat seen during solar maximum is not due to the shorter transit time of the high-speed wind. In other words, one cannot argue that the wave-particle interactions have more time in slower solar wind to scatter the energetic electrons responsible for the majority of the electron heat flux. In fact, the data suggest that the length of the transit time of the wind to the measurement position has no effect on the magnitude of the electron heat flux.

We have also examined the first five years (1990 – 1995) of solar wind and wave data from Ulysses for correlations

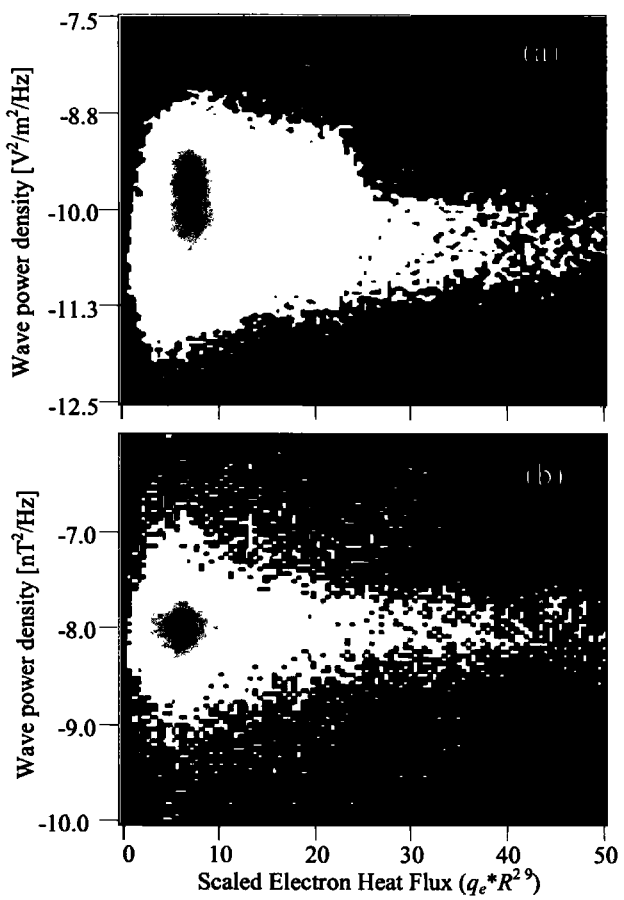

Figure 4. (a) Two dimensional histogram of 18.7 Hz electric field fluctuation power density versus scaled electron heat flux for the years 1990-1995 (solar minimum). Data are binned by heat flux magnitude and electric wave amplitude. The intensity of the grayscale plot corresponds to the number of events falling into each bin. The background level has been set to black to increase the contrast. (b) Two dimensional histogram of 18.7 Hz magnetic field fluctuation power density versus scaled electron heat flux for the years 1990-1995.

between the scaled electron heat flux and either electric field or magnetic field wave activity. The scaled electron heat flux is used to eliminate any correlation due to heliocentric distance, e.g., a general decrease in wave amplitude with increasing heliocentric distance will be distributed amongst all possible values of scaled electron heat flux. Typical results for electric and magnetic correlation studies are shown in Figure 4a and 4b respectively. The data has been binned in both scaled electron heat flux magnitude and wave amplitude. The grayscale level of the points corresponds to the number of events for each pair of electron heat flux magnitude and wave amplitude values and the background level (no measurements) has been set to black to increase the contrast of the figure. All shock intervals have been excluded, the wave frequency is 18.7 Hz (whistler frequency regime), and the wave and electron measurements are required to occur within three minutes of each other. No overall correlation between electron heat flux magnitude and wave amplitude is apparent in either figure. The electric wave data of Figure 4a show a clear absence of large heat flux measurements during periods with large electric wave amplitudes. In contrast, the magnetic wave data shown in Figure 4b show a lack of either intense or weak wave activity during periods corresponding to large heat flux measurements.

4. Discussion

We find that throughout all ten years of Ulysses observations, the electron heat flux obeys a $R^{-2.9}$ scaling. No significant variation in electron heat flux magnitude is seen as a function of heliographic latitude during solar minimum or solar maximum. During both solar maximum and solar minimum, there is no significant correlation between the magnitude of the electron heat flux and the solar wind speed. The universality of this result has important implications for solar wind modeling. For example, in the fast solar wind model of *Hu et al.* [1997] the measured electron temperature at 1 AU forces the authors to artificially lower the electron heat conduction within 1 AU in their model. It would be interesting to see what forms for the electron heat conduction would be required to force such models to match observations at 5 AU.

If heat flux driven instabilities were limiting the heat flux, we would expect that larger values of the scaled q_e should correspond to larger instability growth rates and therefore to larger amplitude fluctuating fields. Figure 4 indicates that electromagnetic instabilities near 18.7 Hz do not play a role in limiting the solar wind heat flux. In particular we conclude, in agreement with *Newbury and Gary* [2001], that the whistler heat flux instability [*Scime et al.*, 1994; *Gary et al.*, 1994] does not provide the observed constraint on the solar wind heat flux.

Given this result and the suggestion of an absence of electrostatic waves during intervals of high electron heat flux, it would be appropriate to seek correlations between q_e and field fluctuation amplitudes at other frequencies beyond the range of the whistler mode. For example, it is still possible that higher frequency, strictly electrostatic, ion acoustic fluctuations [*Hess et al.*, 1998; *Lin et al.*, 2001] may contribute to the regulation of the heat flux.

Acknowledgments. This work was supported by the NASA Heliospheric Mission Guest Investigator Program grant NAG5-6468. We thank the SWOOPS team at LANL and Bruce Goldstein at JPL for processing the raw electron data and the two referees for helpful comments on this manuscript.

References

Bame, S. J., et al., The Ulysses solar wind plasma experiment, *Astron. Astrophys. Suppl. Ser., 92,* 237-266, 1992.

Feldman, W. C., et al., Solar wind electrons, *J. Geophys. Res., 80,* 4181, 1975.

Gary, S. P., et al., The whistler heat flux instability: Threshold conditions in the solar wind, *J. Geophys. Res., 99,* 23,391 1994.

Hess, R. A., et al., Ion acoustic-like waves observed by Ulysses near interplanetary shock waves in the three-dimensional heliosphere, *J. Geophys. Res., 103,* 6531, 1998.

Hollweg, J. V., On electron heat conduction in the solar wind, *J. Geophys. Res., 79,* 3845, 1974.

Hu, Y. Q., et al., A fast solar wind model with anisotropic proton temperature, *J. Geophys. Res., 102,* 14,661, 1997.

Lin, N., et al., Very low frequency waves in the heliosphere: Ulysses Observations, *J. Geophys. Res.*, 103, 12023, 1998.

Lin, N., et al., Ion acoustic waves and their source regions in the solar wind, *J. Geophys. Res.*, submitted, 2001.

Maksimovic, M., V. Pierrand, and J.F. Lemaire, A kinetic model of the solar wind with kappa distribution functions in the corona, *Astron. Astrophys., 324,* 725, 1997.

Maksimovic, S. P. Gary, and R. M. Skoug, Solar wind electron suprathermal strength and temperature gradients: Ulysses observations, *J. Geophys. Res., 105,* 18337, 2001

McComas, D.J., et al., Solar wind observations over Ulysses' first full polar orbit, *J. Geophys. Res., 105,* 10419, 2001a.

McComas, D.J., et al., Ulysses observations of the irregularly structured mid-latitude solar wind during the approach to solar maximum, *Geophys. Res. Lett., 27,* 2437, 2001b.

Meyer-Vernet, N., How does the solar wind blow? A simple kinetic model, *Eur. J. Phys., 20,* 167, 1999.

Newbury, J. A., and S. P. Gary, Whistler instabilities in the solar wind: Magnetic fluctuations and anisotropy constraints, J. Geophys. Res., submitted, 2001.

Pilipp, W. G., et al., Characteristics of electron velocity distribution functions in the solar wind derived from the Helios plasma experiment, *J. Geophys. Res., 92,* 1075, 1987.

Scime, E. E., J. L. Phillips and S. J. Bame, Effects of spacecraft potential on three-dimensional electron measurements in the solar wind, *J. Geophys. Res., 99,* 14769, 1994a.

Scime, E. E., et al., Regulation of the solar wind heat flux from 1 to 5 AU: Ulysses observations, *J. Geophys. Res., 99,* 23,401, 1994b.

Scime, E. E., et al., The electron heat flux in the polar solar wind: Ulysses observations, *Geophys. Res. Lett. 26,* 2129, 1999.

Scudder, J. D. and S. Olbert, A theory of local and global processes which affect solar wind electrons Part 1, *J. Geophys. Res., 84,* 2755, 1979a.

Scudder, J. D. and S. Olbert, A theory of local and global processes which affect solar wind electrons Part 2, *J. Geophys. Res., 84,* 6603, 1979b.

Sittler, E. C., and M. Guhatathakurta, Semiemprical two-dimensional magnetohydrodynamic model of the solar corona and interplanetary medium, *Astrophys. J., 523,* 812, 1999.

Stone, R.G., et al., The Unified Radio and Plasma Wave Investigation, *Astro. Astrophys. Supp. Ser., 92,* 291, 1992.

E. Scime and John E. Littleton, West Virginia University, Morgantown, WV 26506 (e-mail: escime@wvu.edu, jel@wvnvms.wvnet.edu)

S. Peter Gary and R. Skoug, Los Alamos National Laboratory, Los Alamos, NM 87545 (e-mail: pgary@lanl.gov, rskoug@lanl.gov)

N. Lin, University of Minnesota, Minneapolis, MN (e-mail: lin@waves.space.umn.edu)

(Received January 29, 2001; revised March 1, 2001;
accepted March 21, 2001.)